Impact of CO_2 fertilization on maximum foliage cover across the globe's warm, arid environments

Randall J. Donohue,[1] Michael L. Roderick,[2,3,4] Tim R. McVicar,[1] and Graham D. Farquhar[2]

Received 21 March 2013; revised 12 May 2013; accepted 13 May 2013.

[1] Satellite observations reveal a greening of the globe over recent decades. The role in this greening of the "CO_2 fertilization" effect—the enhancement of photosynthesis due to rising CO_2 levels—is yet to be established. The direct CO_2 effect on vegetation should be most clearly expressed in warm, arid environments where water is the dominant limit to vegetation growth. Using gas exchange theory, we predict that the 14% increase in atmospheric CO_2 (1982–2010) led to a 5 to 10% increase in green foliage cover in warm, arid environments. Satellite observations, analyzed to remove the effect of variations in precipitation, show that cover across these environments has increased by 11%. Our results confirm that the anticipated CO_2 fertilization effect is occurring alongside ongoing anthropogenic perturbations to the carbon cycle and that the fertilization effect is now a significant land surface process. **Citation:** Donohue, R. J., M. L. Roderick, T. R. McVicar, and G. D. Farquhar (2013), Impact of CO_2 fertilization on maximum foliage cover across the globe's warm, arid environments, *Geophys. Res. Lett.*, *40*, doi:10.1002/grl.50563.

1. Introduction

[2] Carbon dioxide is a primary substrate of photosynthesis. Increases in atmospheric CO_2 concentrations (C_a) are expected to lead to a CO_2 fertilization effect where photosynthesis is enhanced with the rise in CO_2 [*Farquhar*, 1997]. While a land-based carbon sink has been observed [*Ballantyne et al*., 2012; *Canadell et al*., 2007] and satellites reveal long-term, global greening trends [*Beck et al*., 2011; *Fensholt et al*., 2012; *Nemani et al*., 2003], it has proven difficult to isolate the direct biochemical role of C_a in these trends from variations in other key resources (such as light, water, nutrients [*Field et al*., 1992]) and from socioeconomic factors such as land use change [*Houghton*, 2003]. This complexity can be reduced by focusing on warm, arid environments, where water plays the dominant role in primary production and where foliage cover (F, the fraction of ground area covered by green foliage), plant water use, and photosynthesis are all tightly coupled. It is in these warm, arid environments where the CO_2 fertilization effect on cover should be most clearly expressed. While widespread greening has been reported in these environments [*Beck et al*., 2011; *Fensholt et al*., 2012], the year-to-year variation in precipitation (P) at individual sites makes it very difficult to extract a clear fingerprint of the CO_2 fertilization cover effect.

[3] Global satellite observations show that the relationship of F to P is generally curvilinear (Figure 1a) with a near-linear dependence of F on P under arid conditions (Figure 1b). At low P (i.e., $< \sim 0.4$ m a^{-1}), there is a distinct upper edge that represents the maximum F (F_x) attainable for a given P (Figure 1b). The linearity of the F_x edge highlights the presence of a limit to F when water is the dominant limit to growth. The F_x relation has been previously investigated using the rain-use efficiency (RUE, the ratio of aboveground net primary productivity to P) framework [*Huxman et al*., 2004], and it was found that their upper limit (which is approximately synonymous with our F_x edge) was independent of vegetation and climate types [*Huxman et al*., 2004; *Ponce Campos et al*., 2013]. Leaf-scale gas exchange measurements show that transpiration and photosynthesis are directly coupled to C_a [*Wong et al*., 1979], and this leads us to hypothesize that C_a plays a key role in setting the F_x limit. If this is correct, then we expect that any rise in C_a will produce an increase in the F_x edge. Furthermore, we expect that a first-principles-based estimate of the effect of elevated C_a on cover (which we outline below) will provide an estimate of how much the F_x edge has increased, given the observed rise in C_a (Figure 1b). We test this hypothesis by comparing estimates of changes in F_x with historically observed changes in F_x deduced from satellite observations. This also provides a direct means of observing the CO_2 fertilization cover effect under warm, arid conditions.

2. Predicting the CO_2 Fertilization Cover Effect

[4] The water use efficiency of photosynthesis, W_p, is the ratio of the assimilation (A_l) and transpiration (E_l) rates per unit of leaf area. It is defined as [*Wong et al*., 1979]

$$W_p = \frac{A_l}{E_l} = \frac{C_a}{1.6v}\left(1 - \frac{C_i}{C_a}\right), \tag{1}$$

where C_a and C_i are the atmospheric and intercellular [CO_2], respectively, and v is the leaf-to-air water vapor pressure difference. The relative effect of a change in C_a on W_p is given by

$$\frac{dW_p}{W_p} = \frac{dA_l}{A_l} - \frac{dE_l}{E_l} = \frac{dC_a}{C_a} - \frac{dv}{v} + \frac{d\left(1 - \frac{C_i}{C_a}\right)}{\left(1 - \frac{C_i}{C_a}\right)}. \tag{2}$$

[5] In leaves, *Wong et al*. [1979] showed that C_i/C_a is reasonably conservative for a particular photosynthetic mode

Additional supporting information may be found in the online version of this article.

[1]CSIRO Land and Water, Canberra, ACT, Australia.
[2]Research School of Biology, Australian National University, Canberra, ACT, Australia.
[3]Research School of Earth Sciences, Australian National University, Canberra, ACT, Australia.
[4]Australian Research Council Centre of Excellence for Climate System Science, Sydney, New South Wales, Australia.

Corresponding author: R. J. Donohue, CSIRO Land and Water, GPO Box 1666, Canberra, ACT 2601, Australia. (Randall.Donohue@csiro.au)

0094-8276/13/10.1002/grl.50563

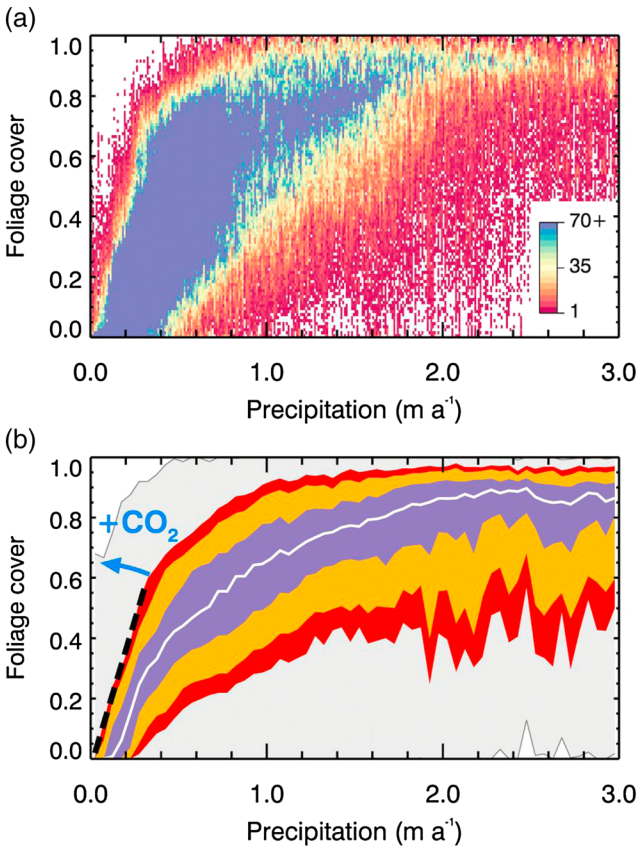

Figure 1. Annual precipitation, foliage cover, and rising CO_2. (a) The relationship between annual precipitation and foliage cover. Global P and F data are 2003 annual values. Colors denote the number of 0.08 degree grid cells across the globe for each P-F combination. Major irrigation areas, lakes, and wetlands have been excluded. (b) Same data as Figure 1a but displayed using percentile bands. That is, we divided the data into 0.02 m a^{-1} P bins, and, for each bin, we identified the 50th percentile F value (white line). We similarly identified the 25th and 75th percentile F values (bottom and top of the purple band, respectively), the 10th and 90th percentiles (bottom of the lower yellow band and top of the upper yellow band, respectively), and the 5th and 95th percentiles (bottom and top of the lower and upper red bands, respectively). The gray area shows the full data range. The black dashed line is the F_x edge, and the blue arrow indicates the expected effect of an increase in C_a on the this edge. F_x values can be artificially enhanced when available water is greater than P (via, for example, irrigation, run-on, or groundwater). Alternatively, when F is less than F_x, factors other than the supply of water prevent foliage cover from reaching the maximum possible value.

(C_3 or C_4) at a given v. However, $(1 - C_i/C_a)$ does increase slightly with increasing v, and the effect has been modeled and observed by taking $(1 - C_i/C_a)$ as being proportional to the square root of v [*Farquhar et al.*, 1993; *Medlyn et al.*, 2011; *Wong and Dunin*, 1987]. With that, equation (2) becomes

$$\frac{dW_p}{W_p} = \frac{dA_l}{A_l} - \frac{dE_l}{E_l} = \frac{dC_a}{C_a} - \frac{1}{2}\frac{dv}{v}. \quad (3)$$

[6] In warm, arid environments, the transpiration per unit ground area (E_g) is constrained by the available water supply (i.e., P) [*Kerkhoff et al.*, 2004; *Specht*, 1972]. Such low-productivity environments typically have a small leaf area index (L, leaf area per unit ground area), and the following approximation is valid [*Lu et al.*, 2003]:

$$E_g \approx E_l L. \quad (4)$$

[7] Our approach examines cover as a function of precipitation. Assuming constant water supply (i.e., constant E_g), we have

$$0 = \frac{dE_l}{E_l} + \frac{dL}{L} \Rightarrow -\frac{dE_l}{E_l} = \frac{dL}{L}. \quad (5)$$

[8] Under warm, arid conditions, L is typically small and F and L vary near proportionally [*Lu et al.*, 2003]. With that, we assume that dL/L and dF/F are approximately equal. For the warm, arid regions being considered, this gives

$$\frac{dW_p}{W_p} \approx \frac{dA_l}{A_l} + \frac{dF}{F} \approx \frac{dC_a}{C_a} - \frac{1}{2}\frac{dv}{v}. \quad (6)$$

[9] Equation (6) provides a quantitative expression linking changes in F with changes in C_a, v, and A_l.

[10] Global satellite observations of F are available from 1982 (see below), and, for the 1982–2010 period, C_a increased by 14% [*P. Tans and R. Keeling*, 2012] (in using a single value of dC_a/C_a, we are assuming that long-term changes in C_a occur uniformly across the globe). For the selected study area (see below), observations show that v increased by ~8% over the same period [*Dee et al.*, 2011], (see supporting information Table S2). This leads to an estimated 10% rise in W_p across the analysis extent (that is, $dC_a/C_a - 1/2 \cdot dv/v$, or $0.14 - 0.08/2$).

[11] If the change in W_p was shared evenly between dA_l/A_l and dF/F, it follows that F would have increased by 5%. Alternatively, in warm, arid regions, leaf area production might be so tightly linked to water availability that the change in C_a (and hence in W_p) might be predominantly expressed through E_l (and hence F), with little change in A_l. In this scenario, dF/F would be around 10%. Thus, our a priori estimate of the CO_2 fertilization effect on F_x in warm, arid regions over the last 30 years is for an increase of 5 to 10%.

3. Observing Changes in the Maximum Cover Edge

[12] To test our hypothesis that the F_x edge is set primarily by C_a, and therefore will increase with the C_a-driven rise in W_p, we quantified the global-scale changes in the F_x edge over the past 30 years using readily available satellite estimates of F [*Tucker et al.*, 2005]. We did this by first restricting our analysis to warm, arid regions where water was the primary limit to vegetation growth. We set an analysis extent (Figure 2) to include only the following areas: (a) areas that were climatically water-limited [*Nemani et al.*, 2003]; (b) areas that were free from irrigation and major surface water features [*Siebert et al.*, 2002; *United Nations Environment Programme*, 2011]; and (c) areas with continuous P data coverage over the study period [*Rudolf et al.*, 2010]. In order to minimize the impact of year-to-year "transient" effects (e.g., soil water storage change and the

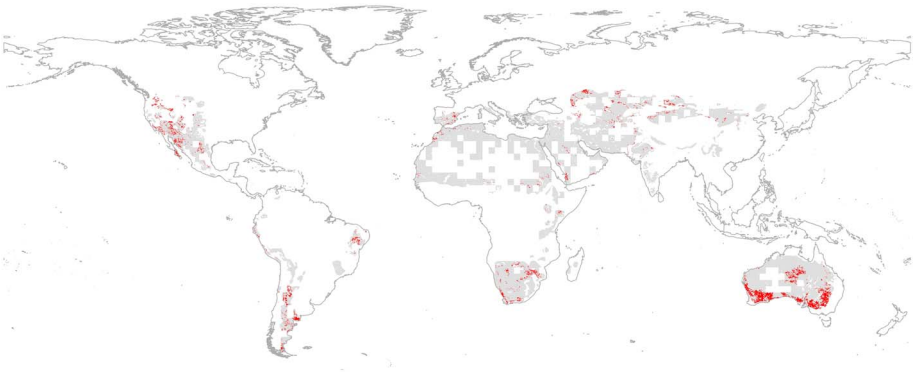

Figure 2. Analysis extent and spatial distribution of the F_x edge. The analysis extent, over which we determined the annual F_x, is shown in gray. Cells within ±5% of the F_x edge for at least one of the 3 year averages are shown in red.

response lag of perennial foliage to changes in P), we performed analyses using sequential 3 year periods (yielding ten 3 year averages between 1982 and 2010, with the last period containing 2 years). Within the analysis extent, and for each 3 year average, we identified the location of the F_x edge by determining the 95th percentile of F for a given P (assessed in 0.02 m a^{-1} bin widths). We then defined the F_x edge as a linear regression fitted to the 95th percentile values that lay between $0.05 \leq F \leq 0.55$. This gave 10 separate estimates of F_x. Finally, we tested whether the slope and intercept of the F_x regression had changed over time. Detailed descriptions of data and methods are presented in the supporting information.

[13] Our findings show that the F_x edge increased between 1982 and 2010 by ~11% (Figure 3a). The change was driven by an increase in the slope of the edge (Figure 3b) with little change in the offset (Figure 3c), consistent with our a priori expectation (Figure 1b). The cells that occur at the F_x edge were distributed across every continent (Figure 2). The ~11% increase observed from the satellite data is close to the upper value a priori estimate—an estimate made by assuming the change in W_p is expressed solely through E_l. This result provides strong support for our hypothesis that the F_x edge is, in large part at least, determined by C_a. By implication (and to the same degree that our hypothesis is correct), analyzing the changes in the F_x edge provides a means of directly observing the CO_2 fertilization effect as it has historically occurred across the globe's warm, arid landscapes.

4. Assessing Alternative Mechanisms of the Rise in the Maximum Cover Edge

[14] Over the study period, average daily air temperature increased [*Dee et al*., 2011], leading to the question of what role, if any, this change may have had in the observed rise in the F_x edge. The impact of changes in air temperature on W_p are explicitly incorporated into our analysis via v (equation (6)), where any temperature-based rise in v will be accompanied by a decrease in W_p and F (and A_l). Hence, higher air temperatures, via the effect on v, have, in our analysis, contributed to a lowering of the F_x edge rather than the observed rise in the edge.

[15] *Huxman et al*. [2004] showed that, regardless of vegetation or climate type, vegetation RUE converges (temporarily) toward a global maximum value (RUE_x) under conditions of severe drought. The F_x edge is nearly synonymous with RUE_x due to F being highly correlated with Aboveground Net Primary Productivity (ANPP) (but F was used here instead as it is much closer to being a direct observation of vegetation than is ANPP). One implication of this global convergence toward the F_x edge is that no individual geographic location lies constantly at the edge but continuously moves in P-F space in response to changes in local conditions. Another implication is that it is possible that an increase in the F_x edge could be caused by changes in the temporal characteristics of drought events and, in particular, by a gradual increase over the period in the severity of the onset of droughts. We tested for an increase in the severity of drought onset events (see supporting information). We found that the initial drop in P at the start of a drought event decreased over time such that the onset severity was smaller by 0.02 m a^{-1} at the end of the period than at the beginning. This trend of a reduction in drought onset severity is consistent with the 10% increase in P across the globe's warm, arid regions (supporting information Table S2) and with other recent analyses of drought [*Sheffield et al*., 2012; *Sun et al*., 2012] and rules out changes in drought conditions as a likely driver of the observed F_x trend.

[16] Across the study area and period, the 10% rise in P has been accompanied by a general greening—a rise in F of 14% (see supporting information Table S2). This P-induced greening cannot explain the rise in the F_x edge, however, for two reasons. First, our analysis technique removed the effects of variability in P; that is, changes in the F_x edge were determined for a constant P. Second, the edge represents the maximum F, rather than the average F, and both *Huxman et al*. [2004] and *Ponce Campos et al*. [2013] suggest that RUE_x *decreases* with an increase in P.

[17] Another alternative mechanism that could potentially explain the observed change in the F_x edge is a change in disturbance regimes. Since an increase in disturbance generally reduces RUE [*Herrmann et al*., 2005; *Prince et al*., 2007; *Seaquist et al*., 2009], it seems plausible that a lessening of the frequency and/or severity of disturbances might lead to an increase in the F_x edge. We argue that this is unlikely for the following two reasons. First, if a location has been disturbed, such that F is lower than its usual "undisturbed" level, it would initially sit well below the F_x edge (i.e., have a depressed RUE). Regrowth of foliage postdisturbance would serve only to bring that location back up toward, and maybe onto, the F_x edge. Second, for disturbance recovery to raise

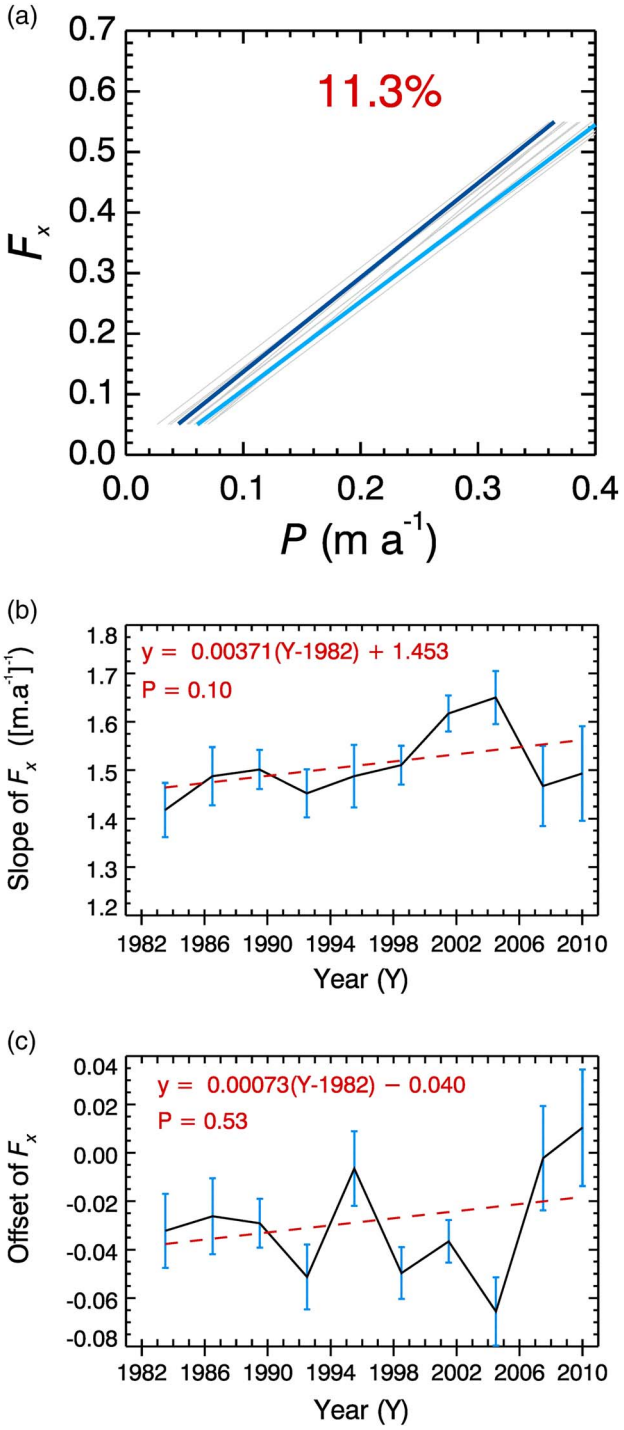

Figure 3. Observed changes in the F_x edge. (a) Results for each of the 3 year averages highlighting the regressed positions of the edge for the 1982–1984 average (light blue) and 2009–2010 average (dark blue). Gray lines show the actual F_x edges identified for each 3 year average and demonstrate the variability in the edge locations. Red text shows the percent change in F_x for the upper end of the edge. The 95% confidence interval for the change at the upper end of the edge is −9 to +27%. (b and c) The changes in the slope and intercept, respectively, of the F_x edge. Bars denote the standard error of the regression coefficients. The dashed line and equation describe the fitted linear trend. P values were derived using the nonparametric, two-sided Kendall-tau test.

the F_x edge, it would require that *all* locations across the analysis extent were initially in a synchronized postdisturbance recovery phase such that the F_x edge was suppressed *globally* at the start of the period. Only then would the gradual increase in postdisturbance cover be able to shift a global growth limit (i.e., the F_x edge). We are not aware of evidence to suggest that such a scenario has occurred.

5. Conclusion

[18] The increase in water use efficiency of photosynthesis with rising C_a has long been anticipated to lead to increased foliage cover in warm, arid environments [*Berry and Roderick*, 2002; *Bond and Midgley*, 2000; *Farquhar*, 1997; *Higgins and Scheiter*, 2012], and both satellite and ground observations from the world's rangelands reveal widespread changes toward more densely vegetated and woodier landscapes [*Buitenwerf et al.*, 2012; *Donohue et al.*, 2009; *Knapp and Soule*, 1996; *Morgan et al.*, 2007; *Scholes and Archer*, 1997]. Our results suggest that C_a has played an important role in this greening trend and that, where water is the dominant limit to growth, cover has increased in direct proportion to the CO_2-driven rise in W_p. This CO_2 fertilization cover effect warrants consideration as an important land surface process.

[19] The results reported here for warm, arid regions do not simply translate to other environments where alternative resource limitations (e.g., light, nutrients, temperature) might dominate, although the underlying theory remains valid (equations (1)–(3)). The remaining challenges are to develop a more general understanding of how the increase in C_a is shared between A_l and E_l in environments that are not warm and arid and to develop capacity to quantify the multiple potential flow-on effects of fertilization in these environments, such as widespread changes in surface albedo, an increase in fire fuel loads for a given P, and possible reductions in stream flows due to enhanced rooting systems [*Buitenwerf et al.*, 2012].

[20] Overall, our results confirm that the direct biochemical impact of the rapid increase in C_a over the last 30 years on terrestrial vegetation is an influential and observable land surface process.

[21] **Acknowledgments.** We thank A.P. O'Grady, J.G. Canadell, and P.B. Hairsine for comments on early versions of the manuscript. We are grateful to J.E. Pinzon and C.J. Tucker for providing the GIMMS 3g NDVI data set. R.J.D. and T.R.M. acknowledge the support of CSIRO's Sustainable Agriculture Flagship and Water for a Healthy Country Flagship. M.L.R acknowledges support from the Australian Research Council (CE11E0098, DP110105376). G.D.F. acknowledges support from the Australian Research Council (DP110105376) and Land & Water Australia.

[22] The Editor thanks two anonymous reviewers for their assistance in evaluating this paper.

References

Ballantyne, A. P., C. B. Alden, J. B. Miller, P. P. Tans, and J. W. C. White (2012), Increase in observed net carbon dioxide uptake by land and oceans during the past 50 years, *Nature*, *488*(7409), 70–72, doi:10.1038/nature11299.

Beck, H. E., T. R. McVicar, A. I. J. M. van Dijk, J. Schellekens, R. A. M. de Jeu, and L. A. Bruijnzeel (2011), Global evaluation of four AVHRR-NDVI data sets: Intercomparison and assessment against Landsat imagery, *Remote Sens. Environ.*, *115*(10), 2547–2563, doi:10.1016/j.rse.2011.05.012.

Berry, S. L., and M. L. Roderick (2002), CO_2 and land-use effects on Australian vegetation over the last two centuries, *Aust. J. Bot.*, *50*(4), 511–531.

Bond, W. J., and G. F. Midgley (2000), A proposed CO_2-controlled mechanism of woody plant invasion in grasslands and savannas, *Global Change Biol.*, *6*(8), 865–869.

Buitenwerf, R., W. J. Bond, N. Stevens, and W. S. W. Trollope (2012), Increased tree densities in South African savannas: >50 years of data suggests CO_2 as a driver, *Global Change Biol.*, *18*(2), 675–684, doi:10.1111/j.1365-2486.2011.02561.x.

Canadell, J. G., C. Le Quere, M. R. Raupach, C. B. Field, E. T. Buitenhuis, P. Ciais, T. J. Conway, N. P. Gillett, R. A. Houghton, and G. Marland (2007), Contributions to accelerating atmospheric CO_2 growth from economic activity, carbon intensity, and efficiency of natural sinks, *Proc. Natl. Acad. Sci. U. S. A.*, *104*(47), 18866–18870, doi:10.1073/pnas.0702737104.

Dee, D. P., et al. (2011), The ERA-Interim reanalysis: Configuration and performance of the data assimilation system, *Q. J. R. Meteorol. Soc.*, *137*(656), 553–597, doi:10.1002/qj.828.

Donohue, R. J., T. R. McVicar, and M. L. Roderick (2009), Climate-related trends in Australian vegetation cover as inferred from satellite observations, 1981–2006, *Global Change Biol.*, *15*(4), 1025–1039, doi:10.1111/j.1365-2486.2008.01746.x.

Farquhar, G. D. (1997), Carbon dioxide and vegetation, *Science*, *278*(5342), 1411.

Farquhar, G. D., J. Lloyd, J. A. Taylor, L. B. Flanagan, J. P. Syvertsen, K. T. Hubick, S. C. Wong, and J. R. Ehleringer (1993), Vegetation effects on the isotope composition of oxygen in atmospheric CO_2, *Nature*, *363*(6428), 439–443, doi:10.1038/363439a0.

Fensholt, R., et al. (2012), Greenness in semi-arid areas across the globe 1981–2007—An Earth Observing Satellite based analysis of trends and drivers, *Remote Sens. Environ.*, *121*, 144–158, doi:10.1016/j.rse.2012.01.017.

Field, C. B., F. S. Chapin, P. A. Matson, and H. A. Mooney (1992), Responses of terrestrial ecosystems to the changing atmosphere—A resource-based approach, *Annu. Rev. Ecol. Syst.*, *23*, 201–235.

Herrmann, S. M., A. Anyamba, and C. J. Tucker (2005), Recent trends in vegetation dynamics in the African Sahel and their relationship to climate, *Global Environ. Change-Human Policy Dim.*, *15*(4), 394–404.

Higgins, S. I., and S. Scheiter (2012), Atmospheric CO_2 forces abrupt vegetation shifts locally, but not globally, *Nature*, *488*(7410), 209–212, doi:10.1038/nature11238.

Houghton, R. A. (2003), Revised estimates of the annual net flux of carbon to the atmosphere from changes in land use and land management 1850–2000, *Tellus, Ser. B*, *55*(2), 378–390, doi:10.1034/j.1600-0889.2003.01450.x.

Huxman, T. E., et al. (2004), Convergence across biomes to a common rain-use efficiency, *Nature*, *429*(6992), 651–654.

Kerkhoff, A. J., S. N. Martens, and B. T. Milne (2004), An ecological evaluation of Eagleson's optimality hypotheses, *Funct. Ecol.*, *18*(3), 404–413.

Knapp, P. A., and P. T. Soule (1996), Vegetation change and the role of atmospheric CO_2 enrichment on a relict site in central Oregon: 1960–1994, *Ann. Assoc. Am. Geogr.*, *86*(3), 387–411.

Lu, H., M. R. Raupach, T. R. McVicar, and D. J. Barrett (2003), Decomposition of vegetation cover into woody and herbaceous components using AVHRR NDVI time series, *Remote Sens. Environ.*, *86*(1), 1–18.

Medlyn, B. E., R. A. Duursma, D. Eamus, D. S. Ellsworth, I. C. Prentice, C. V. M. Barton, K. Y. Crous, P. de Angelis, M. Freeman, and L. Wingate (2011), Reconciling the optimal and empirical approaches to modelling stomatal conductance, *Global Change Biol.*, *17*(6), 2134–2144, doi:10.1111/j.1365-2486.2010.02375.x.

Morgan, J. A., D. G. Milchunas, D. R. LeCain, M. West, and A. R. Mosier (2007), Carbon dioxide enrichment alters plant community structure and accelerates shrub growth in the shortgrass steppe, *Proc. Natl. Acad. Sci. U. S. A.*, *104*(37), 14724–14729, doi:10.1073/pnas.0703427104.

Nemani, R. R., C. D. Keeling, H. Hashimoto, W. M. Jolly, S. C. Piper, C. J. Tucker, R. B. Myneni, and S. W. Running (2003), Climate-driven increases in global terrestrial net primary production from 1982 to 1999, *Science*, *300*(5625), 1560–1563.

Ponce Campos, G. E., et al. (2013), Ecosystem resilience despite large-scale altered hydroclimatic conditions, *Nature*, *494*(7437), 349–352, doi:10.1038/nature11836.

Prince, S. D., K. J. Wessels, C. J. Tucker, and S. E. Nicholson (2007), Desertification in the Sahel: A reinterpretation of a reinterpretation, *Global Change Biol.*, *13*(7), 1308–1313.

Rudolf, B., A. Becker, U. Schneider, A. Meyer-Christoffer, and M. Ziese (2010), GPCC Status Report 7 pp., Global Precip. Climatol. Cent., Offenbach, Germany.

Scholes, R. J., and S. R. Archer (1997), Tree-grass interactions in savannas, *Annu. Rev. Ecol. Syst.*, *28*, 517–544, doi:10.1146/annurev.ecolsys.28.1.517.

Seaquist, J. W., T. Hickler, L. Eklundh, J. Ardo, and B. W. Heumann (2009), Disentangling the effects of climate and people on Sahel vegetation dynamics, *Biogeosciences*, *6*(3), 469–477.

Sheffield, J., E. F. Wood, and M. L. Roderick (2012), Little change in global drought over the past 60 years, *Nature*, *491*(435–438), doi:10.1038/nature11575.

Siebert, S., P. Döll, and J. Hoogeveen (2002), Global map of irrigated areas, version 2.1, Cent. for Environ. Syst. Res., Univ. of Kassel, Kassel, Germany.

Specht, R. L. (1972), Water use by perennial evergreen plant communities in Australia and Papua New Guinea, *Aust. J. Bot.*, *20*(3), 273–299.

Sun, F. B., M. L. Roderick, and G. D. Farquhar (2012), Changes in the variability of global land precipitation, *Geophys. Res. Lett.*, *39*, L19402, doi:10.1029/2012GL053369.

Tans, P., and R. Keeling (2012), Trends in atmospheric Carbon Dioxide, www. esrl. noaa. gov/gmd/eegg/trends/.

Tucker, C. J., J. E. Pinzon, M. E. Brown, D. A. Slayback, E. W. Pak, R. Mahoney, E. F. Vermote, and N. El Saleous (2005), An extended AVHRR 8-km NDVI dataset compatible with MODIS and SPOT vegetation NDVI data, *Int. J. Remote Sens.*, *26*(20), 4485–4498.

United Nations Environment Programme (2011), UNEP Environmental Data Explorer, http://geodata.grid.unep.ch, Geneva, Switzerland.

Wong, S. C., and F. X. Dunin (1987), Photosynthesis and transpiration of trees in a Eucalypt forest stand: CO_2, light and humidity responses, *Aust. J. Plant Physiol.*, *14*(6), 619–632.

Wong, S. C., I. R. Cowan, and G. D. Farquhar (1979), Stomatal conductance correlates with photosynthetic capacity, *Nature*, *282*(5737), 424–426.